NATIONAL ADVISORY COMMITTEE FOR AERONAUTICS

TECHNICAL NOTE 4079

WIND-TUNNEL INVESTIGATION OF EXTERNAL-FLOW JET-AUGMENTED DOUBLE SLOTTED FLAPS ON A RECTANGULAR WING AT AN ANGLE OF ATTACK OF 0° TO HIGH MOMENTUM COEFFICIENTS

By Edwin E. Davenport

Langley Aeronautical Laboratory
Langley Field, Va.

Washington
September 1957

NATIONAL ADVISORY COMMITTEE FOR AERONAUTICS

TECHNICAL NOTE 4079

WIND-TUNNEL INVESTIGATION OF EXTERNAL-FLOW JET-AUGMENTED DOUBLE SLOTTED FLAPS ON A RECTANGULAR WING AT AN ANGLE OF ATTACK OF 0° TO HIGH MOMENTUM COEFFICIENTS

By Edwin E. Davenport

SUMMARY

A preliminary investigation of external-flow jet-augmented double slotted flaps on a rectangular wing with an aspect ratio of 6 has been made in the Langley 300 MPH 7- by 10-foot tunnel. High-momentum air was blown from one and two nacelles over the double slotted flaps of 30 percent wing chord incorporating vanes of either 58.3 percent or 20 percent of the flap chord.

Lift coefficients larger than the jet reaction in the lift direction were attained with the external-flow jet-augmented double slotted flaps. Over the lift-coefficient range investigated, these flaps produced about 80 percent of the lift produced by the jet-augmented plain flap investigated in NACA Technical Note 3865. The lift coefficients for configurations incorporating an inboard nacelle, a midspan nacelle, or twin nacelles were about the same throughout the momentum-coefficient range tested.

With the center of moments at 25 percent wing mean aerodynamic chord, large negative pitching moments were found to exist for the double-slotted-flap configurations which were comparable with those produced by the jet-augmented plain flap previously investigated. The loss in lift needed to trim these pitching moments for a tail located 2 wing chords behind the wing was estimated to range from 7.5 percent to 27.5 percent of the total wing lift.

INTRODUCTION

Considerable emphasis is being placed on methods of increasing the lift of airplane wings to reduce the landing and take-off distances and velocities. One such method, which employs the jet flap, consists of directing a thin, high-momentum, jet sheet of air downward from a continuous slot in the wing trailing-edge region (ref. 1) and, thus, greatly augments

the lifting capabilities of a wing. Investigations (refs. 2 and 3) in which the air was ejected from a slot on the upper surface of the wing and thence downward over a round trailing edge indicated even greater lift augmentation. Another arrangement of the jet-augmented flap (ref. 4) in which the exhaust from pod-mounted jet engines was deflected upward through a slot between the wing and flap and then downward over the flap also showed promise in augmenting the lift of wings.

The present investigation was undertaken to determine the lift-augmentation abilities of an external-flow jet-augmented flap in which the jet exhaust from pod-mounted nacelles is directed over a double slotted flap. This configuration was chosen because it is better lift-wise in the event of power failure than the single slotted flap of reference 4.

This preliminary investigation of external-flow jet-augmented flaps was conducted on a rectangular wing with an aspect ratio of 6 with double slotted flaps in the Langley 300 MPH 7- by 10-foot tunnel. High-momentum air was blown from one and two nacelles, suspended below the wing, over double slotted flaps of 30 percent chord. The investigation covered a momentum-coefficient range from 0 to 28 and a flap-deflection range from 45° to 90° at an angle of attack of 0°.

SYMBOLS

The coefficients of forces and moments are referred to the wind axes with the center of moments at 25 percent wing mean aerodynamic chord.

C_D drag coefficient, $\frac{\text{Drag}}{qS}$

C_L lift coefficient, $\frac{\text{Lift}}{qS}$

$C_{L,\Gamma}$ jet-circulation lift coefficient

$(C_L)_{C_\mu=0}$ jet-off lift coefficient

C_m pitching-moment coefficient, $\frac{M}{qS\bar{c}}$

C_μ momentum coefficient, $\frac{w_j V_j}{gqS}$

c	wing chord, ft
$\bar{c}$	wing mean aerodynamic chord, 0.833 ft for wing with aspect ratio of 6
g	acceleration due to gravity, 32.2 ft/sec^2
M	pitching moment, ft-lb
F_i	measured thrust at engine nacelle, lb
F_r	measured jet reaction with flaps deflected, lb
p	free-stream static pressure, lb/sq ft
p_t	total pressure at nozzle exit, lb/sq ft
q	free-stream dynamic pressure, $\frac{\rho V^2}{2}$, lb/sq ft
ρ	mass density of air, slugs/cu ft
R	universal gas constant, $\frac{\text{ft-lb}}{\text{lb}}\Big/{}^{\circ}\text{R}$
S	semispan-wing area, 2.083 sq ft for wing with aspect ratio of 6
α	angle of attack, deg
T	nozzle-exit temperature, $^{\circ}$R
V	free-stream velocity, ft/sec
V_j	jet velocity (isentropic expansion is assumed), $\sqrt{\frac{2\gamma}{\gamma - 1} RTg\left[1 - \left(\frac{p}{p_t}\right)^{\frac{\gamma-1}{\gamma}}\right]}$, ft/sec
w_j	weight rate of jet flow, lb/sec
γ	ratio of specific heats for air, 1.4
δ_f	flap-deflection angle, measured with respect to wing chord line, deg
δ_j	jet-deflection angle, measured with respect to wing chord line, deg

APPARATUS AND MODEL

The external-flow jet-augmented double slotted flaps were investigated in the Langley 300 MPH 7- by 10-foot tunnel by means of the semispan-wing technique in which the ceiling of the tunnel was used as the reflection plane. The general arrangement of the wing, flaps, and nacelles is shown in figures 1 and 2. The 10-inch-chord NACA 0012 airfoil was modified behind the 0.6c station to allow for the installation of the double slotted flaps (fig. 1). The semispan wing was unswept and untapered and had a span of 30 inches. The large-vane double-slotted-flap configuration consisted of a flap of 30 percent of the wing chord made of steel and a vane of 58.3 percent of the flap chord made of aluminum. A small steel vane of 20 percent of the flap chord was used with the 30-percent-chord flap for the small-vane double-slotted-flap configuration. The vane ordinates are given in tables I and II and the flap ordinates are given in table III. The nacelles used with the double slotted flaps were constructed from standard $1\frac{1}{4}$- inch steel pipe with a 1-inch-diameter orifice at the exit (figs. 1 and 2).

High-pressure air was brought to the balance frame by means of the same piping arrangement used in the investigation of reference 2. A $1\frac{1}{4}$-inch steel pipe, rigidly attached to the balance frame, projected through a tunnel-ceiling slot and supported the nacelles in the proximity of the wing. The weight rate of air flow was determined by means of a calibrated sharp-edged orifice in the air-supply pipe.

TESTS AND TEST CONDITIONS

The tests were made in the Langley 300 MPH 7- by 10-foot tunnel at the dynamic pressures, velocities, Reynolds numbers, and momentum-coefficient ranges given in the following table:

Dynamic pressure, q, lb/sq ft	Velocity, V, ft/sec	Reynolds number	Range of momentum coefficient, C_μ
1	29.2	154,000	0 to 28.00
2	41.3	218,000	0 to 17.38
10	92.4	488,000	0 to 3.49

The most desirable condition would have been to conduct all the tests at the highest dynamic pressure of 10 pounds per square foot.

However, since the air supply available was limited to about 1.04 pounds per second at 300 pounds per square inch, it became necessary to use lower values of dynamic pressure to cover a higher momentum-coefficient range.

Three nacelle arrangements were tested with the large-vane double-slotted-flap configuration: a twin-nacelle arrangement with nacelles at the 27-percent- and 76-percent-semispan stations, a single inboard nacelle at the 27-percent-semispan station, and a midspan nacelle at the 50-percent-semispan station. Only the twin-nacelle arrangement was tested with the small-vane double slotted flap.

The large-vane double slotted flap was tested through a flap-deflection range from 45° to 90°, and the small-vane double slotted flap was tested through a flap-deflection range from 45° to 75°. All tests were conducted with the wing at an angle of attack of 0°.

CORRECTIONS

Jet-boundary corrections applied to the drag data were obtained from the methods of reference 5. The angle of attack was not corrected. The magnitude of the corrections was determined by considering only the aerodynamic forces (circulation-lift effects) on the model that resulted after the jet-reaction components had been subtracted from the data as follows:

$$C_D = C_{D,\text{measured}} + 0.00357\left[C_L - C_\mu \sin\left(\delta_j + \alpha\right)\right]^2$$

As a result of the small size of the model with respect to the size of the tunnel test section, blocking corrections were believed to be negligible and, thus, were not applied to the data. Tare corrections were applied to lift, drag, and pitching moment to account for the effect of nacelle piping. These corrections were measured in the absence of the wing. Because the investigation was of a preliminary nature, the mutual wing-pipe interference effects were not determined.

RESULTS AND DISCUSSION

Presentation of Results

Static calibration of the effectiveness of the flaps in turning the jet downward is presented in figures 3, 4, and 5. A sample plot of the

factors making up the lift coefficient of the large-vane external-flow jet-augmented double-slotted-flap configuration at $\delta_f = 75^\circ$ is presented as figure 6. The longitudinal aerodynamic coefficients at zero angle of attack for the twin-nacelle configurations are presented as a function of lift coefficient in figures 7 and 8 for the large- and small-vane configurations, respectively. A comparison of the aerodynamic characteristics of the two double-slotted-flap configurations with those of a jet-augmented plain flap from reference 2 is given in figure 9. A comparison of the longitudinal aerodynamic coefficients of single- and twin-nacelle configurations at zero angle of attack on the large-vane double slotted flap is presented in figure 10.

Discussion

Tests with $q = 0$.- A measure of the flap effectiveness in turning the jet downward F_r/F_i determined from the lift and drag data with zero tunnel velocity is presented as a function of the initial jet reaction (thrust) F_i in figure 3. The large-vane flap configuration redirected approximately 69 percent of the initial jet reaction about 56° at $\delta_f = 45^\circ$, but only 56 percent was redirected 90° when $\delta_f = 75^\circ$. One possible explanation of these low efficiencies is that part of the initial reaction is lost in the spanwise flow which occurs when the jet strikes the flaps. The small-vane-configuration data (fig. 3(b)) generally show about the same values of F_r/F_i as those of the large-vane-configuration data at the lower flap deflections, but about 10 percent less at a flap deflection of 75°.

The jet-deflection angle obtained from lift and drag measurements was generally about 12° larger than the flap-deflection angle. (See fig. 4.) The jet-deflection angle is influenced by the curvature of the upper surface of the flap which forms an angle of 18° with the flap reference line at the flap trailing edge. As noted in reference 6, the jet-deflection angle computed from lift and drag values, measured on the balance system at $q = 0$, includes induced components arising from pressures induced on the wing and flap by the jet. Since a pressure distribution over the wing and flap was not included in this investigation, the magnitude of these effects could not be determined.

In reducing the data in this paper, the calculated thrust of the nacelle has been used $\left(w_j V_j/g\right)$. The losses associated with the nacelle exit are shown in figure 5 which compares the calculated and measured values of thrust in the absence of the wing and shows that the measured values are about 10 percent less than the calculated values. This difference should be kept in mind when comparing these data with data based on a measured value of thrust.

Lift coefficient.- The lift coefficient of a wing with a jet flap can be divided into three separate components as follows:

$$C_L = (C_L)_{C_\mu=0} + C_\mu \sin(\delta_j + \alpha) + C_{L,\Gamma}$$

where $(C_L)_{C_\mu=0}$ is the jet-off lift coefficient, $C_\mu \sin(\delta_j + \alpha)$ is the jet-reaction component in the lift direction, and $C_{L,\Gamma}$ is the pressure-lift coefficient induced by the jet sheet.

The variation of these components with C_μ for the large-vane double-slotted-flap configuration is shown in figure 6. This variation, which is typical of all the configurations investigated, shows that lift coefficients larger than the jet reaction in the lift direction were obtained with the external-flow jet-augmented double slotted flap. The momentum coefficients ranged from 0 to 28 and the lift coefficients varied from about 1.2 to 28 as can be seen from a study of the figures. The jet-reaction component in the lift direction $C_\mu \sin(\delta_j + \alpha)$ shown in figure 6 is based on the calculated momentum coefficients available at the nacelle exit. Since this analysis does not take into account the spanwise losses which occur as the jet spreads over the flaps or the 10-percent difference between calculated and measured thrust at the nacelle exit, the value of $C_{L,\Gamma}$ shown is conservative; the analysis does show, however, the gain that is obtained with this arrangement over that of directing the jet downward at an angle equal to δ_j.

The variation of C_L with δ_f for the double-slotted-flap arrangement (figs. 7 and 8) is not as pronounced as for the jet flap of reference 2, probably because of the decrease in jet-deflection efficiency (fig. 3) with increased double-slotted-flap deflection. In fact, there is only a small variation with deflection for the small-vane configuration (fig. 8(a)). The largest values of C_L obtained over most of the C_μ range were at $\delta_f = 75^\circ$ $(\delta_j = 90^\circ)$ for the large-vane configuration and at $\delta_f = 55^\circ$ $(\delta_j = 66^\circ)$ for the small-vane configuration (figs. 8 and 9).

Both of the twin-nacelle double-slotted-flap configurations are compared in figure 9 with the jet-augmented plain flap of reference 2 on the basis of equivalent angles of δ_j. Over the range of C_μ investigated, the large- and small-vane double slotted flaps produced lift coefficients amounting to about 80 percent and 75 percent, respectively, of the lift coefficients produced by the jet-augmented plain flap. In making this comparison it should be remembered that both the configurations in this investigation and in the one reported in reference 2 were of a preliminary nature, and the configurations were not necessarily optimum.

Nacelle location and the number of nacelles used was seen to have no appreciable effect on the lift characteristics at low values of C_μ (fig. 10) but began to have an effect at the upper limits of the range of C_μ. For instance, in the range of C_μ from 10 to 17 the twin-nacelle configuration clearly produces higher lift coefficients for a given value of C_μ than either of the single-nacelle configurations.

Drag characteristics.- Since the drag coefficient includes the jet-reaction component in the thrust direction, the drag coefficient shows a pronounced variation with δ_f at a constant lift coefficient. For example, at a lift coefficient of 20 the drag coefficient varies from -5.7 at $\delta_f = 45^\circ$ to 9.5 at $\delta_f = 90^\circ$ (fig. 7(b)). The drag coefficients throughout the lift-coefficient range for the twin-nacelle configuration were generally lower than those for the inboard-nacelle configuration (fig. 10). Increasing the number of nacelles improved the spanwise distribution of the jet and decreased the drag values.

Pitching-moment characteristics.- The pitching-moment data show that, as for the jet flap (refs. 1 and 2), the large lift coefficients associated with jet-augmented flaps are accompanied by large pitching moments. The results of both the large- and small-vane configurations (figs. 7 and 8, respectively) indicate a decrease in pitching-moment coefficient with increased flap deflection. Similar trends are shown in reference 2 for a wing with a very short flap chord.

If a tail length of $2\bar{c}$ is assumed, the loss in lift due to the tail load required to trim out the negative pitching moment of the wing measured at $0.25\bar{c}$ for the large- and small-vane double-slotted-flap configurations varied from 22.5 to 27.5 percent and from 7.5 to 19.25 percent, respectively, of the total wing lift. Corresponding values for the jet-augmented plain flap were from 10.0 to 19.75 percent of the total wing lift.

SUMMARY OF RESULTS

A wind-tunnel investigation has been made of external-flow jet-augmented double slotted flaps on a rectangular wing at an angle of attack of 0° to high momentum coefficients, and the following results are presented:

1. Lift coefficients larger than the jet reaction in the lift direction were obtained with the external-flow jet-augmented double slotted flaps.

2. Over the lift-coefficient range from 1.2 to 28 and the momentum-coefficient range from about 0 to 28, the average lift coefficients obtained with the large- and small-vane external-flow double slotted jet-augmented flaps were about 80 percent and 75 percent, respectively, of the lift coefficients attainable with a jet-augmented plain flap.

3. With the center of moments at the 25 percent mean aerodynamic chord, large negative pitching moments were found to exist for the external-flow jet-augmented double slotted flaps. The loss in lift required to trim these pitching moments was estimated to be from 7.5 percent to 27.5 percent of the total wing lift which is comparable with that of a jet-augmented plain flap.

4. The variation of lift coefficient with momentum coefficient was about the same for an inboard nacelle, a midspan nacelle, or a twin-nacelle configuration.

Langley Aeronautical Laboratory,
National Advisory Committee for Aeronautics,
Langley Field, Va., June 6, 1957.

REFERENCES

1. Williams, J., and Alexander, A. J.: Three-Dimensional Wind-Tunnel Tests of a 30° Jet Flap Model. Rep. No. F.M. 2326, British N.P.L. (Rep. No. 17,990, A.R.C.), Nov. 1955.

2. Lockwood, Vernard E., Turner, Thomas R., and Riebe, John M.: Wind-Tunnel Investigation of Jet-Augmented Flaps on a Rectangular Wing to High Momentum Coefficients. NACA TN 3865, 1956.

3. Lowry, John G., and Vogler, Raymond D.: Wind-Tunnel Investigation at Low Speeds To Determine the Effect of Aspect Ratio and End Plates on a Rectangular Wing With Jet Flaps Deflected 85°. NACA TN 3863, 1956.

4. Campbell, John P., and Johnson, Joseph L, Jr.: Wind-Tunnel Investigation of an External-Flow Jet-Augmented Slotted Flap Suitable for Application to Airplanes With Pod-Mounted Engines. NACA TN 3898, 1956.

5. Gillis, Clarence L., Polhamus, Edward C., and Gray, Joseph L., Jr.: Charts for Determining Jet-Boundary Corrections for Complete Models in 7- by 10-Foot Closed Rectangular Wind Tunnels. NACA WR L-123, 1945. (Formerly NACA ARR L5G31.)

6. Malavard, L., Poisson-Quinton, Ph., and Jousserandot, P. (T. M. Berthoff and D. C. Hazen, trans.): Theoretical and Experimental Investigations of Circulation Control. Rep. No. 358, Princeton Univ., Dept. Aero. Eng., July 1956.

TABLE I.- LARGE-VANE ORDINATES

[All dimensions are in inches]

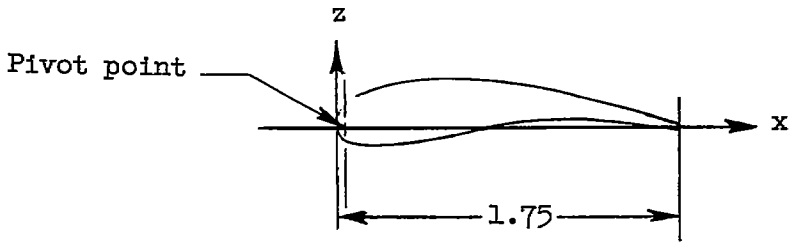

Station, x	Upper z	Lower z
0	0	0
.075	.128	-.106
.100	.142	-.109
.125	.153	-.111
.150	.164	-.113
.250	.197	-.111
.350	.219	-.100
.450	.232	-.084
.550	.236	-.062
.650	.235	-.036
.750	.228	-.010
.850	.218	.010
.950	.203	.024
1.050	.185	.032
1.150	.165	.036
1.250	.144	.038
1.350	.119	.036
1.450	.093	.030
1.550	.065	.020
1.650	.034	.005
1.750	.003	-.012
Pivot-point ordinates: x = 0.04, z = 0		

TABLE II.- SMALL-VANE ORDINATES

[All dimensions are in inches]

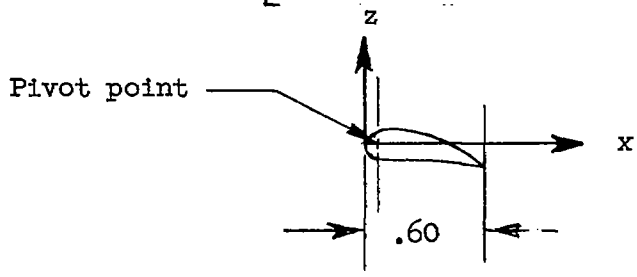

Station, x	Upper z	Lower z
0	0	0
.010	.030	-.029
.020	.043	-.042
.030	.051	-.049
.040	.058	-.054
.050	.063	-.059
.060	.068	-.063
.070	.072	-.066
.080	.075	-.068
.090	.077	-.069
.100	.080	-.070
.150	.080	-.063
.200	.074	-.054
.250	.064	-.047
.300	.050	-.040
.350	.032	-.040
.400	.012	-.043
.450	-.011	-.052
.500	-.037	-.064
.550	-.066	-.080
.600	-.097	-.097
Pivot-point ordinates: x = 0.04, z = 0		

TABLE III.- FLAP ORDINATES

[All dimensions are in inches]

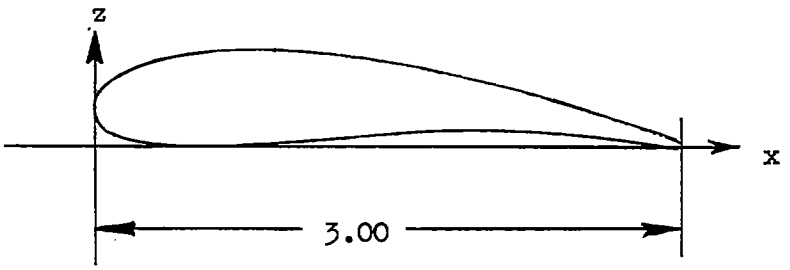

Station, x	Upper z	Lower z
0	0.190	0.1902
.150	.361	.0369
.300	.424	.0099
.450	.460	0
.600	.479	.0009
.750	.487	.0060
.900	.488	.0150
1.050	.481	.0249
1.200	.466	.0381
1.350	.448	.0522
1.500	.425	.0672
1.650	.398	.0801
1.800	.368	.0882
1.950	.335	.0891
2.100	.302	.0891
2.250	.260	.0831
2.400	.217	.0720
2.550	.170	.0582
2.700	.120	.0411
2.850	.067	.0201
3.000	.007	.0069

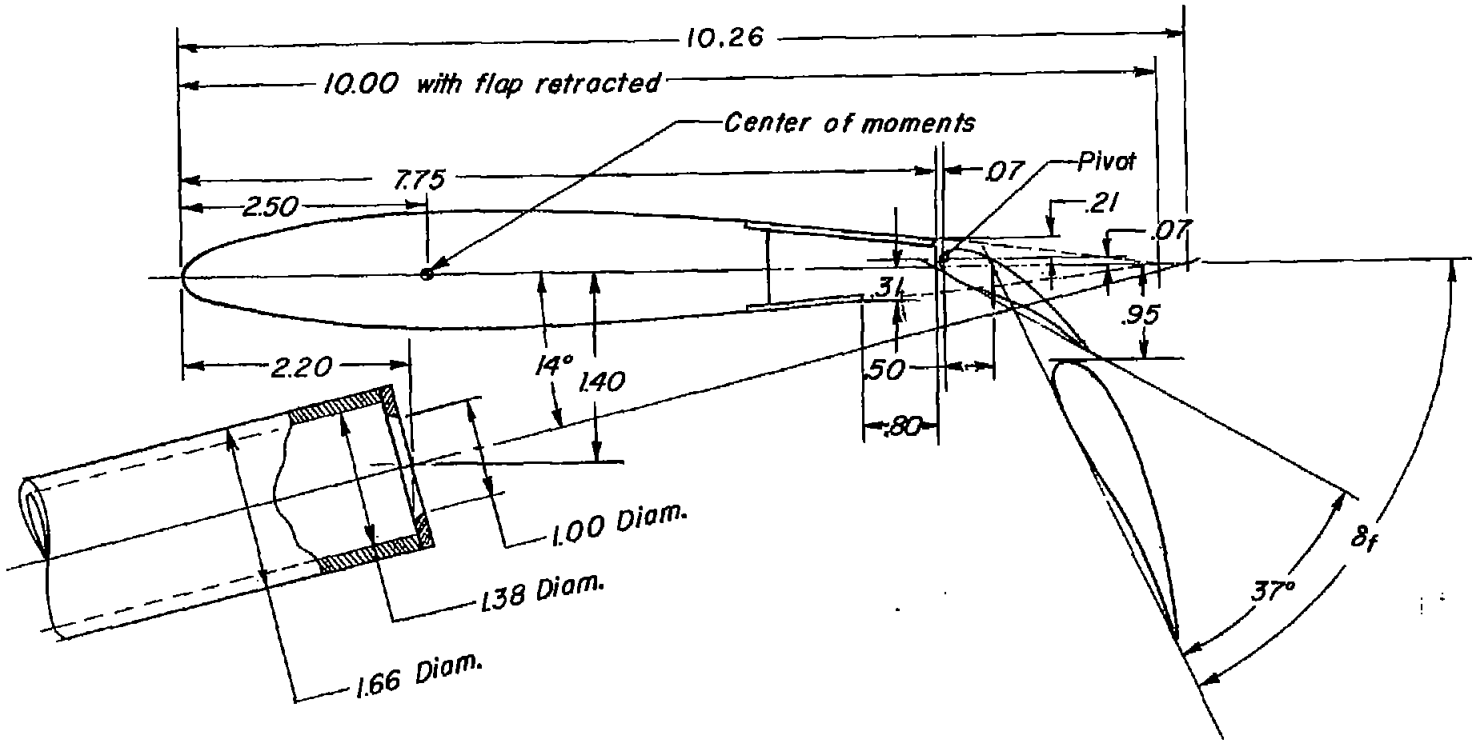

(a) Large-vane configuration. Flap of 30 percent of wing chord with vane of 58.3 percent of flap chord.

Figure 1.- Details of external-flow jet-augmented double slotted flap investigated on a rectangular wing with an aspect ratio of 6 having an NACA 0012 airfoil section. All dimensions are in inches.

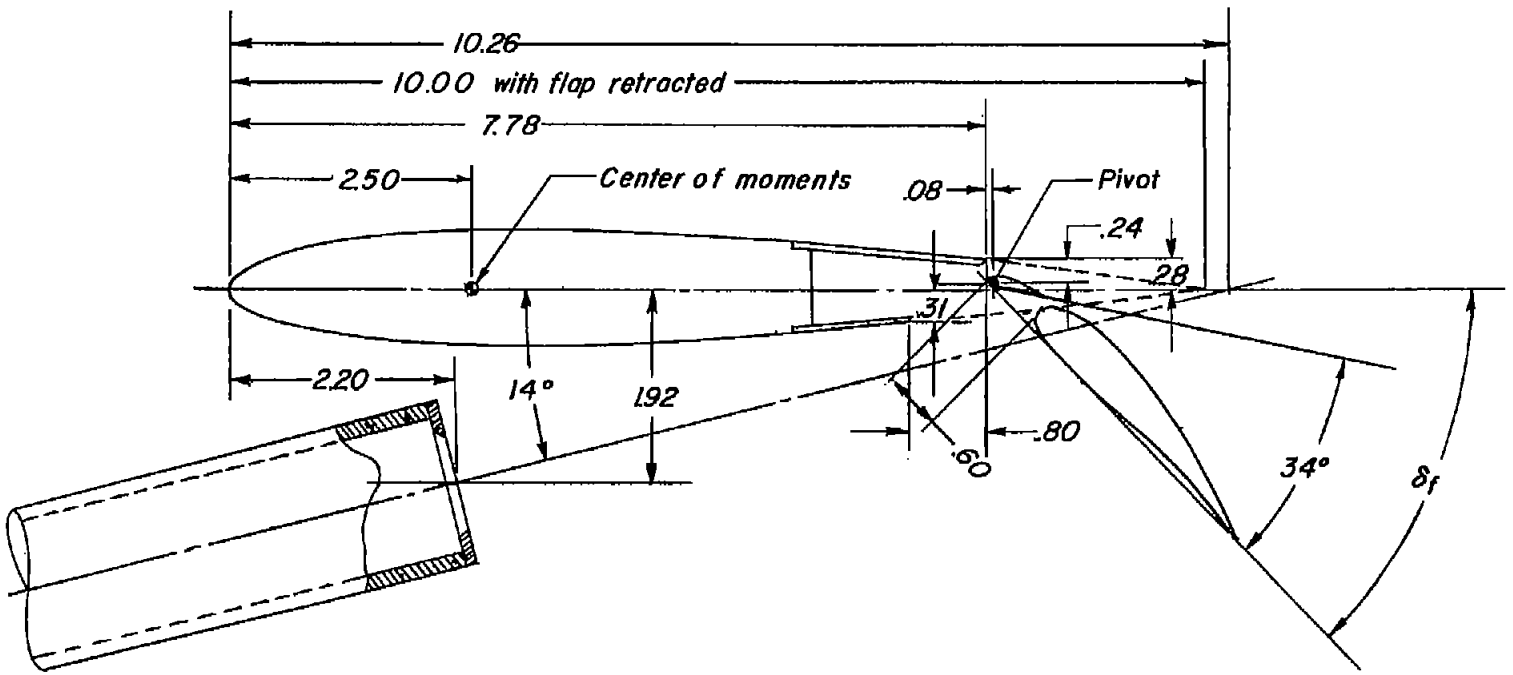

(b) Small-vane configuration. Flap of 30 percent of wing chord with vane of 20 percent of flap chord.

Figure 1.- Concluded.

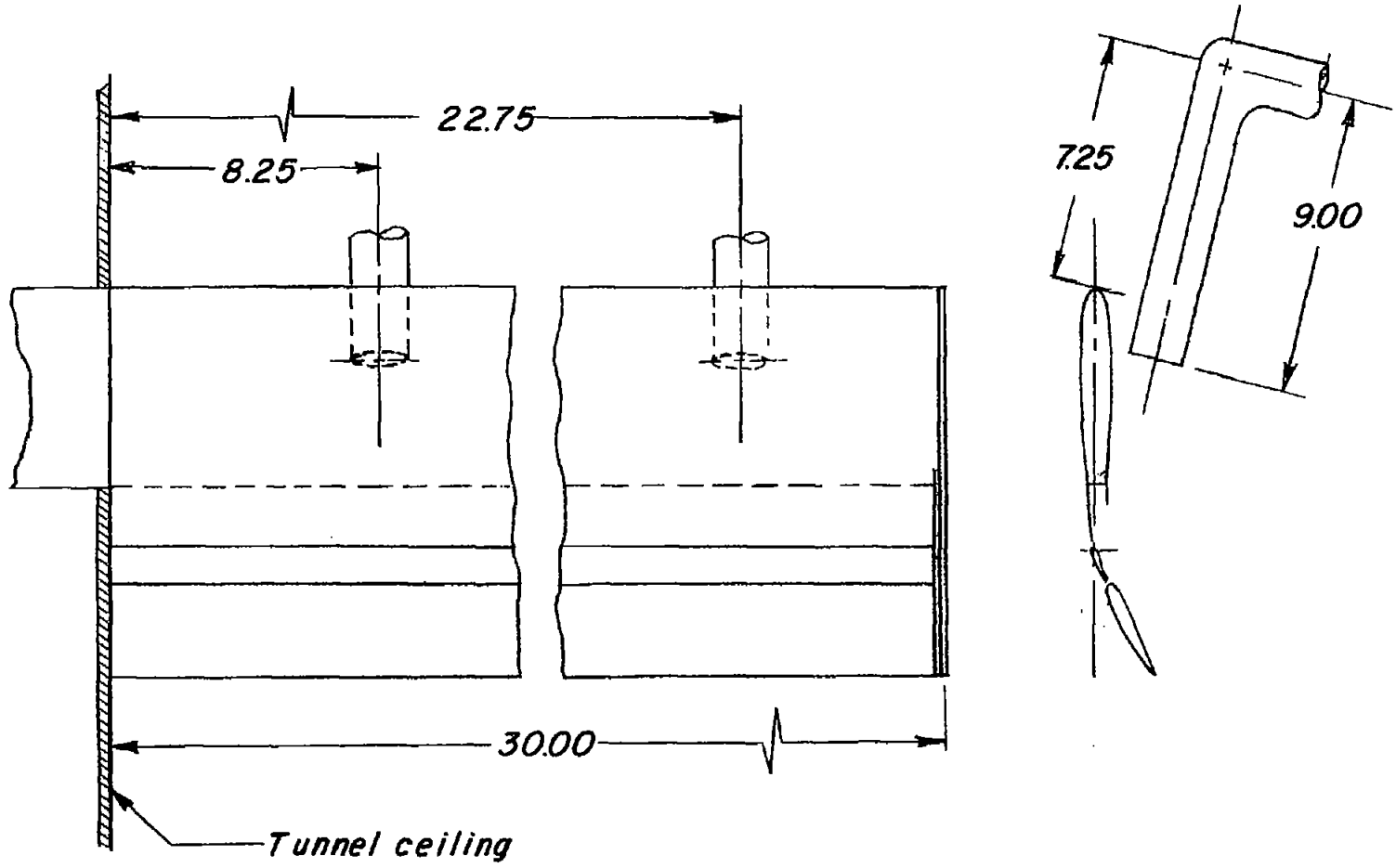

Figure 2.- Spanwise location of nacelles for double slotted flaps and proximity of nacelle support tube. All dimensions are in inches.

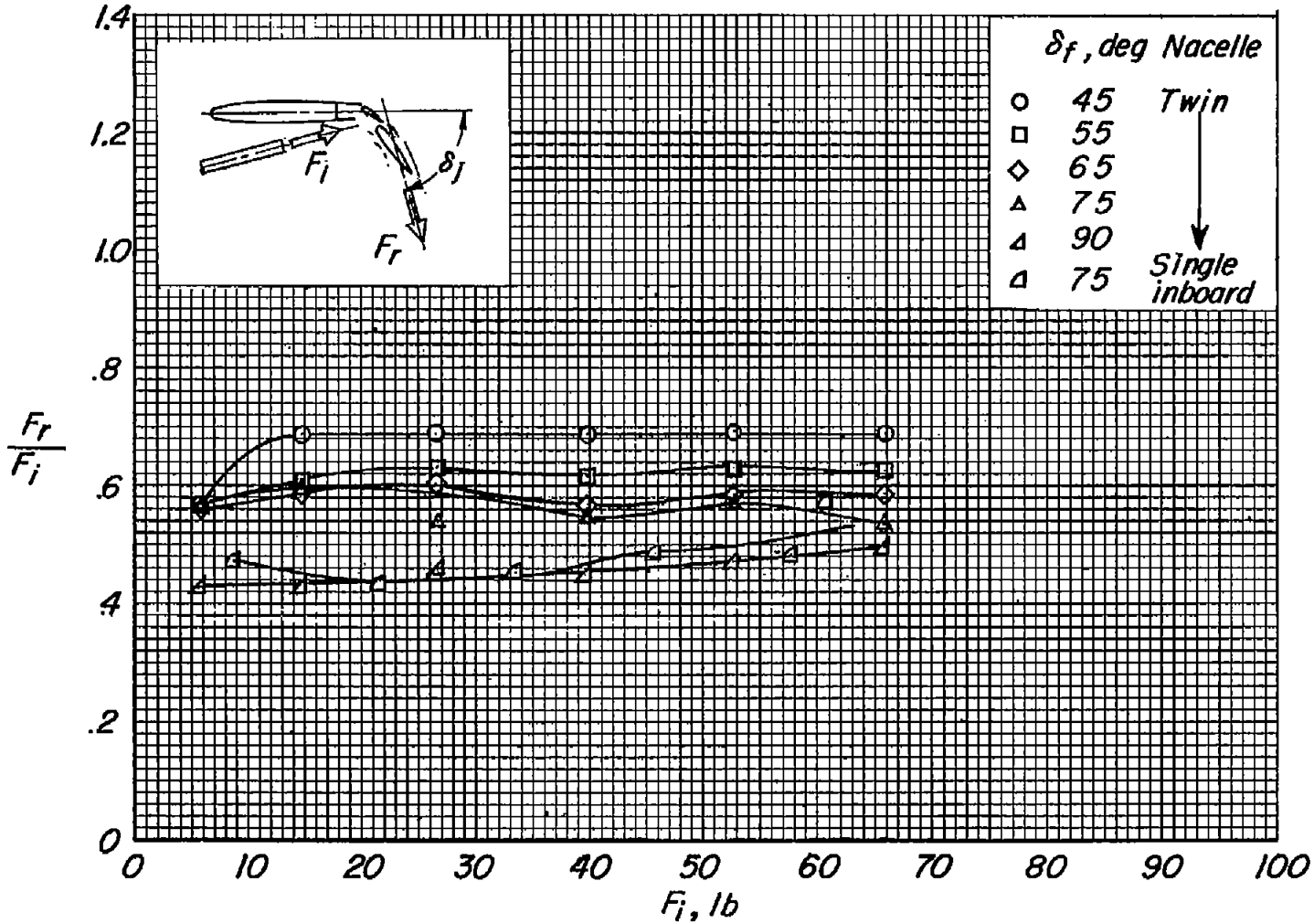

(a) Large-vane configuration. Twin- and inboard-nacelle arrangements.

Figure 3.- Effect of flap-deflection angle on jet-deflection effectiveness. q = 0.

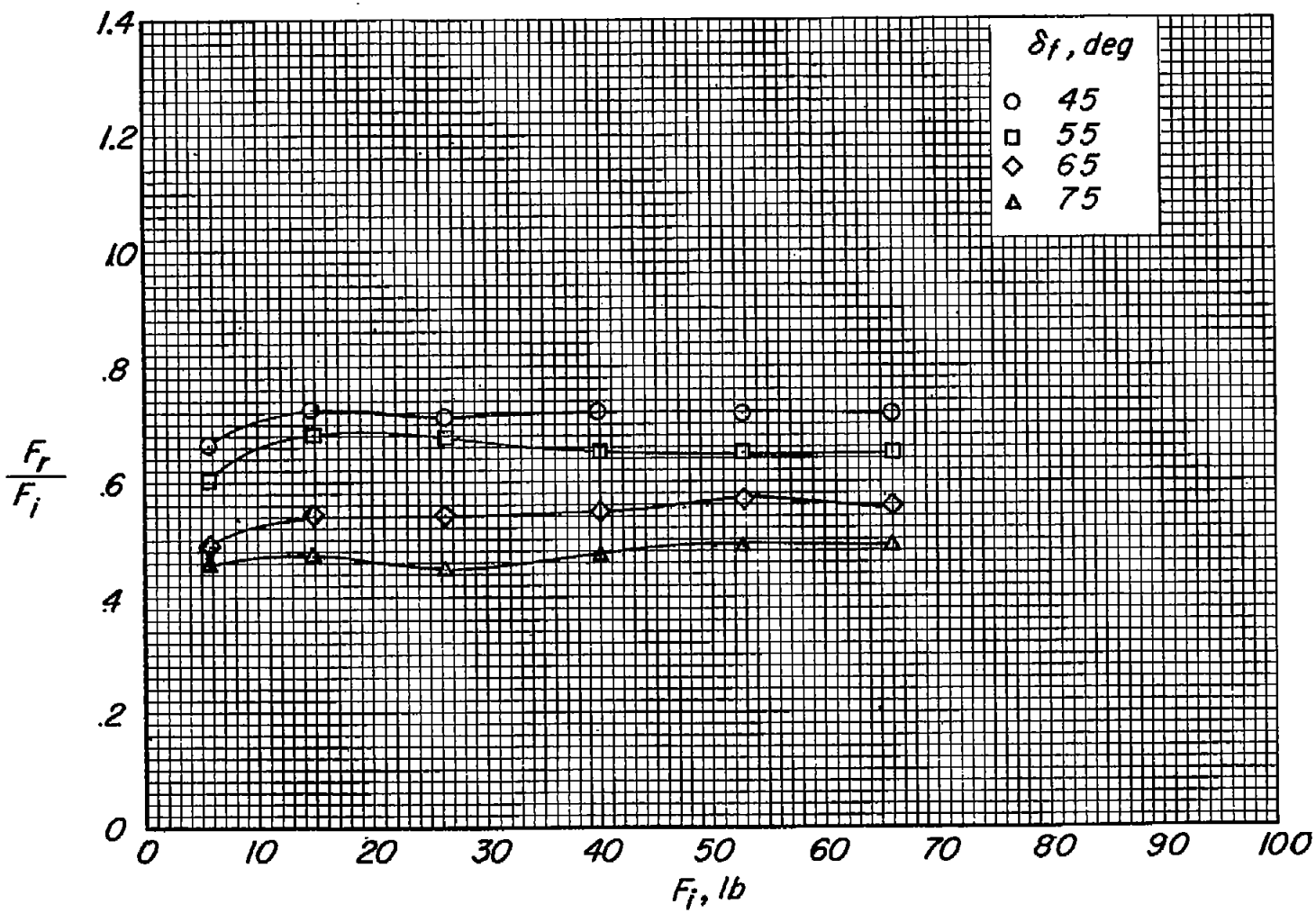

(b) Small-vane configuration. Twin-nacelle arrangement.

Figure 3.- Concluded.

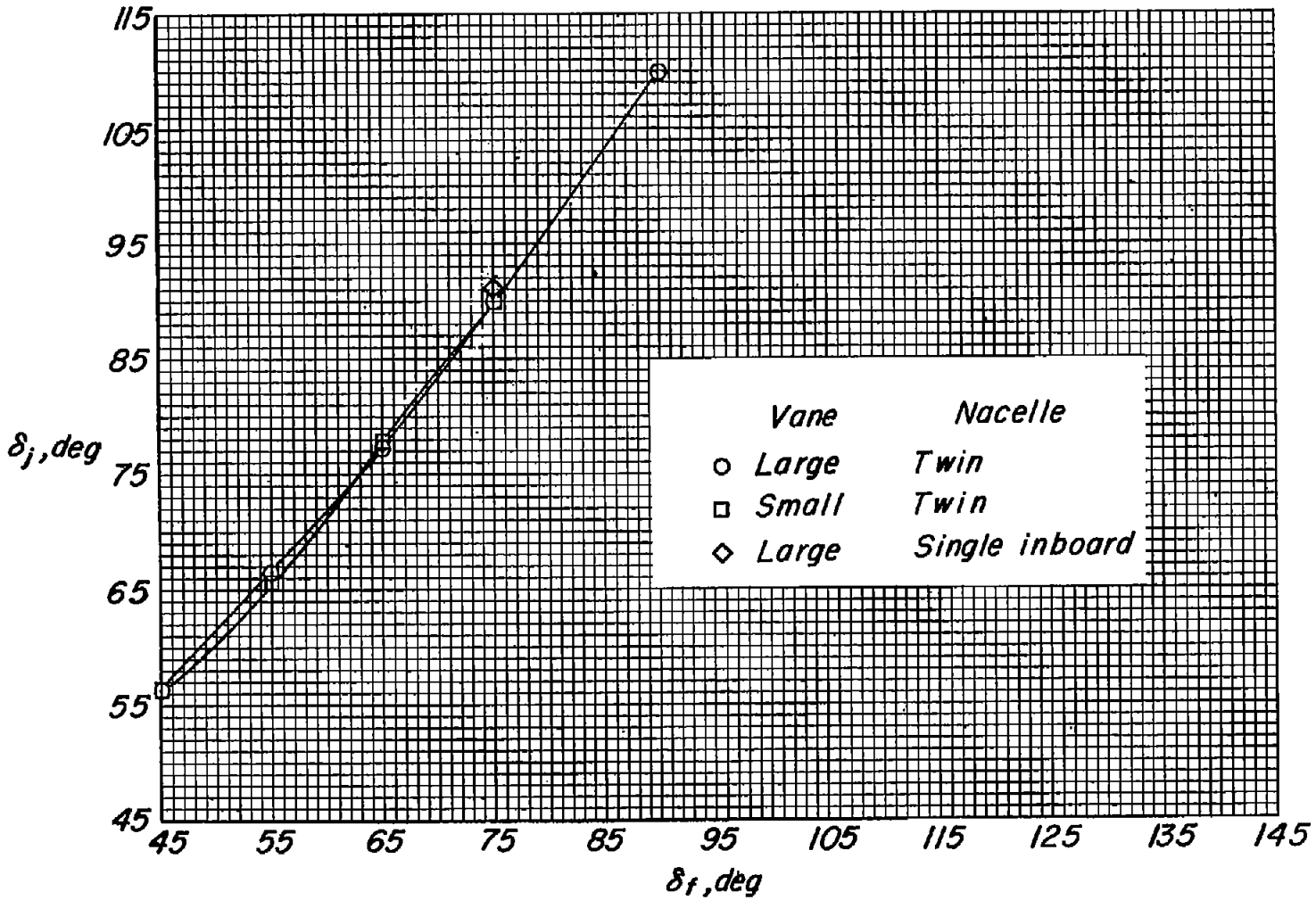

Figure 4.- Variation of jet-deflection angle with flap-deflection angle for large- and small-vane configurations. $q = 0$.

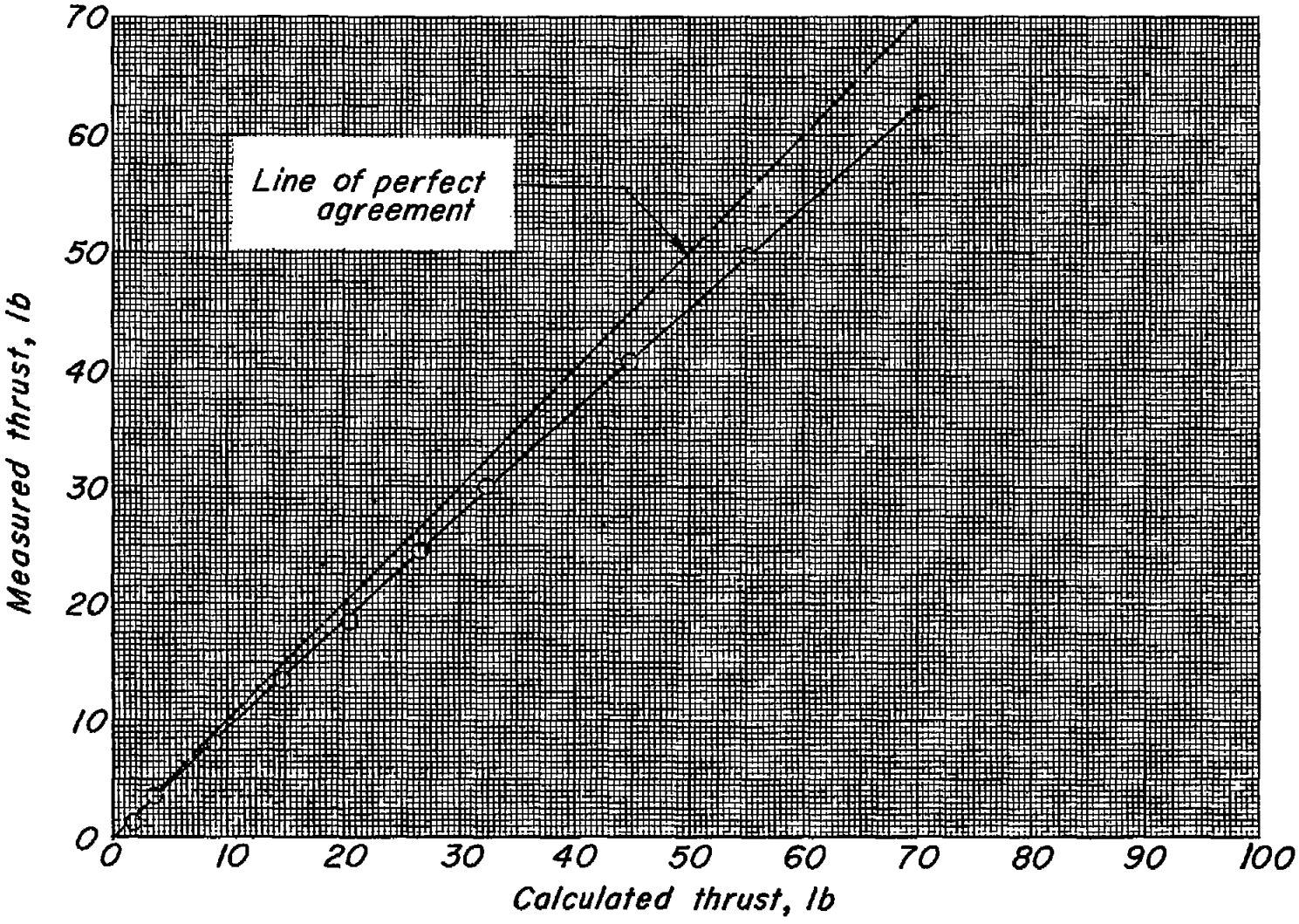

Figure 5.- Variation of calculated thrust with measured thrust obtained in absence of wing.

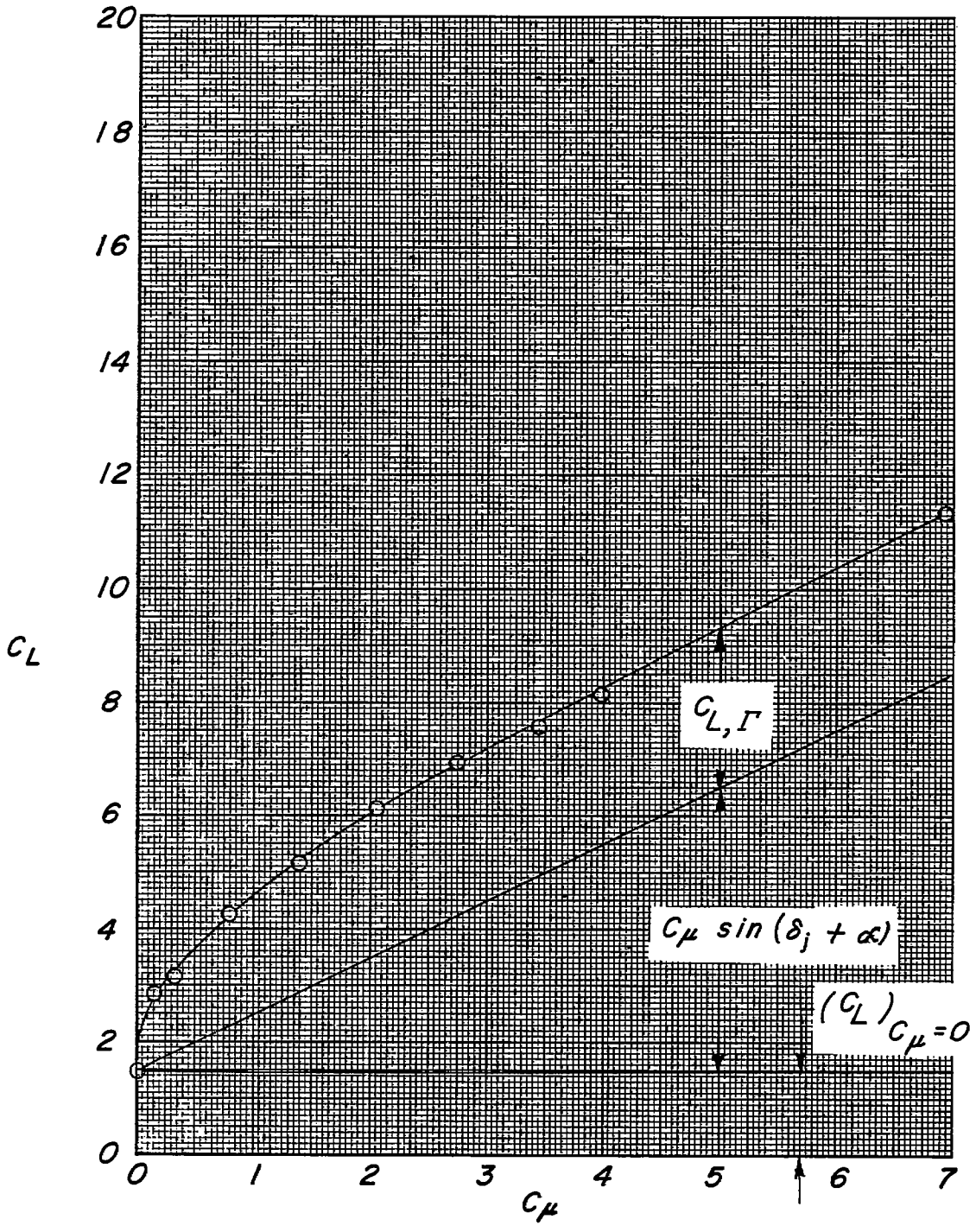

Figure 6.- Factors making up the lift coefficient of the large-vane double-slotted-flap configuration.

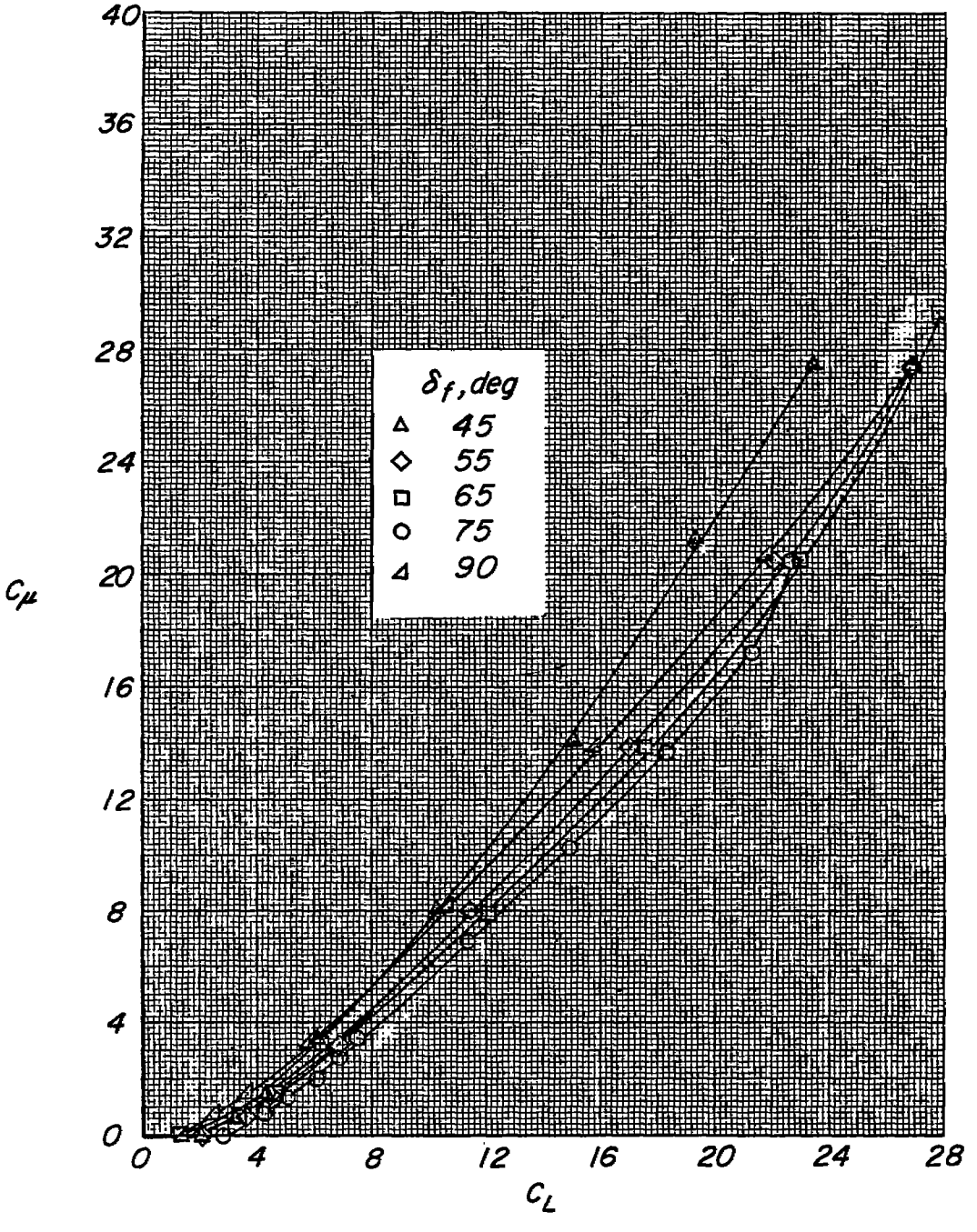

(a) Variation of C_μ with C_L for various flap-deflection angles.

Figure 7.- Aerodynamic effects of blowing from the twin-nacelle arrangement over a large-vane double-slotted-flap configuration. $\alpha = 0^\circ$.

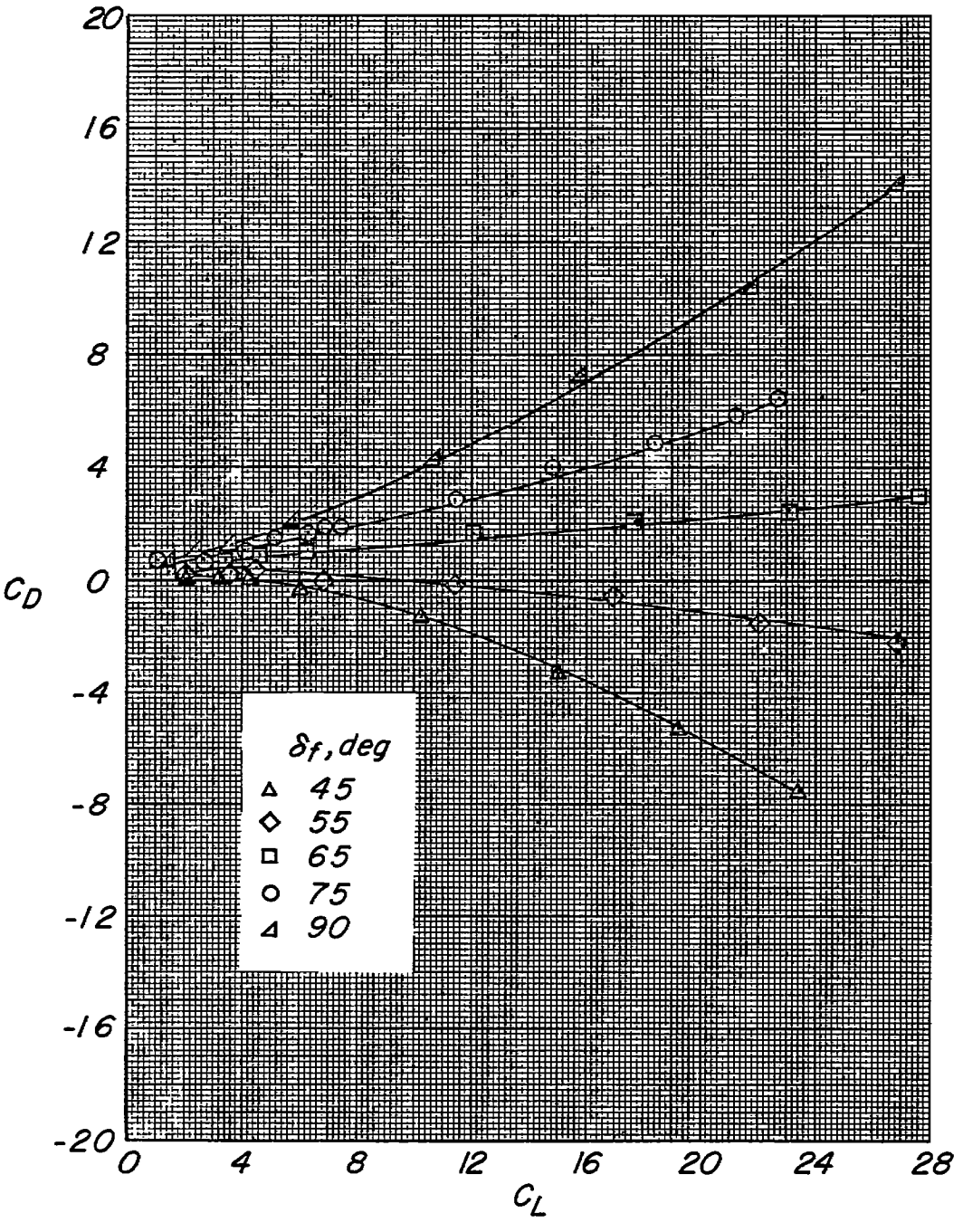

(b) Variation of C_D with C_L for various flap-deflection angles.

Figure 7.- Continued.

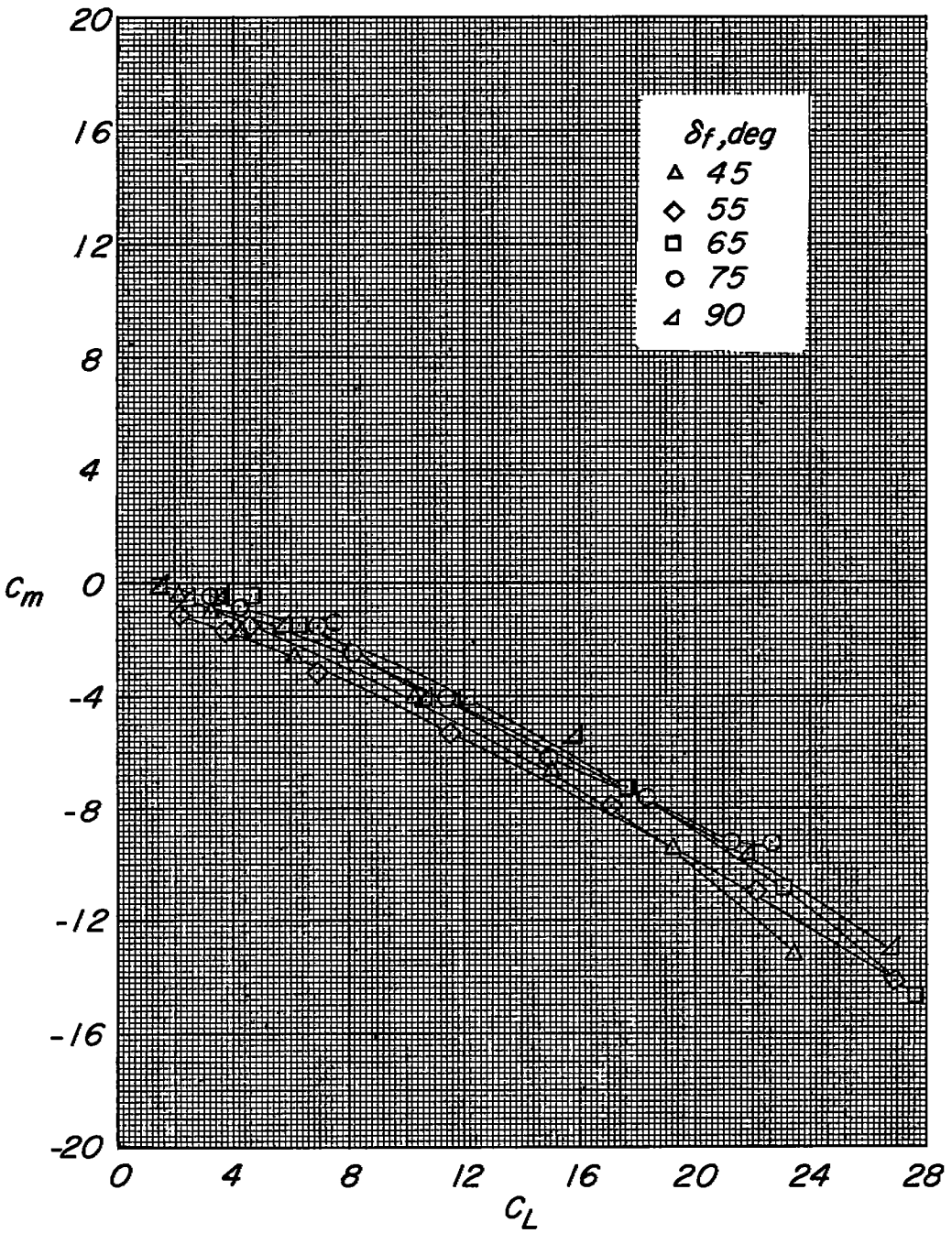

(c) Variation of C_m with C_L for various flap-deflection angles.

Figure 7.- Concluded.

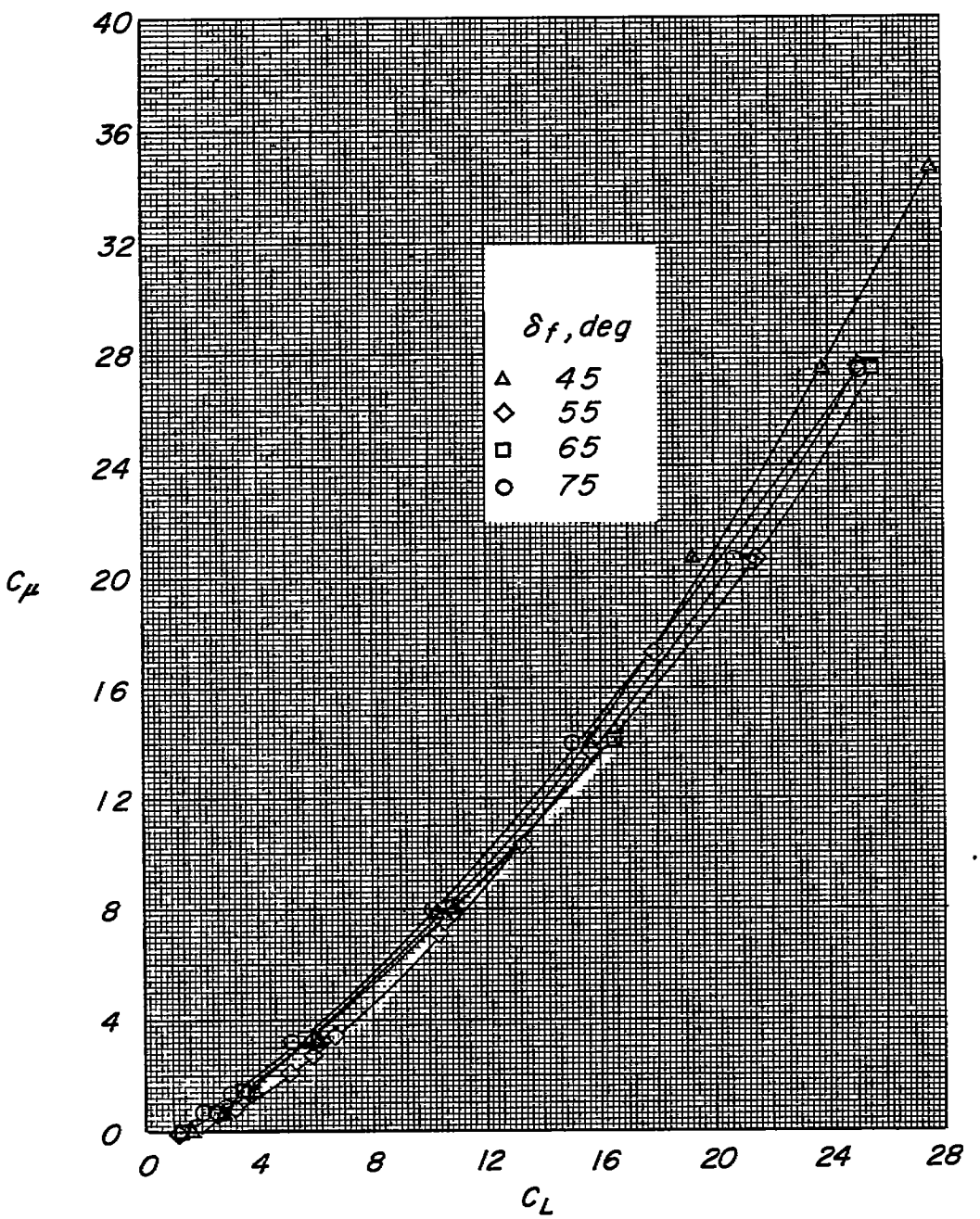

(a) Variation of C_μ with C_L for various flap-deflection angles.

Figure 8.- Aerodynamic effects of blowing from the twin-nacelle arrangement over a small-vane double-slotted-flap configuration. $\alpha = 0^\circ$.

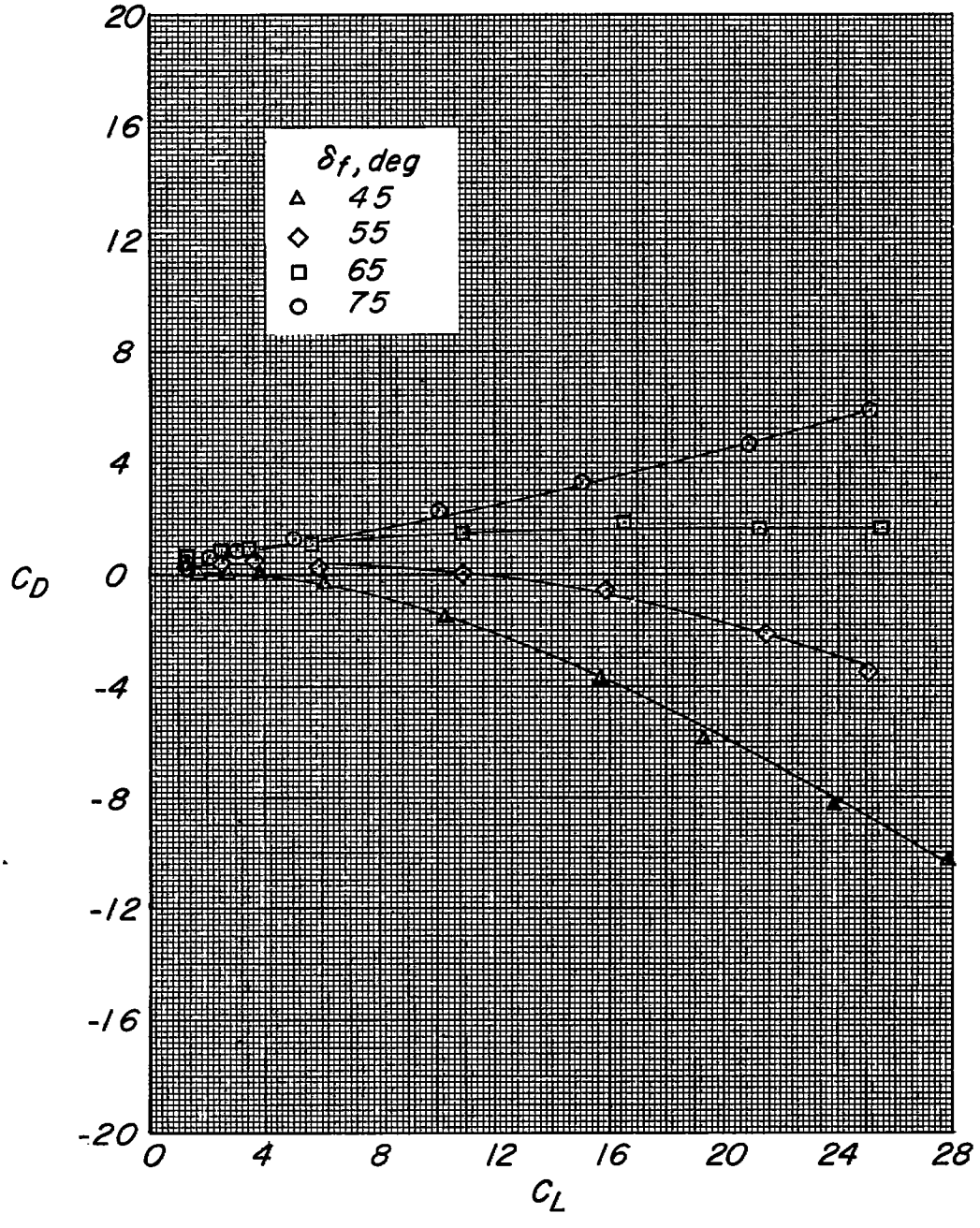

(b) Variation of C_D with C_L for various flap-deflection angles.

Figure 8.- Continued.

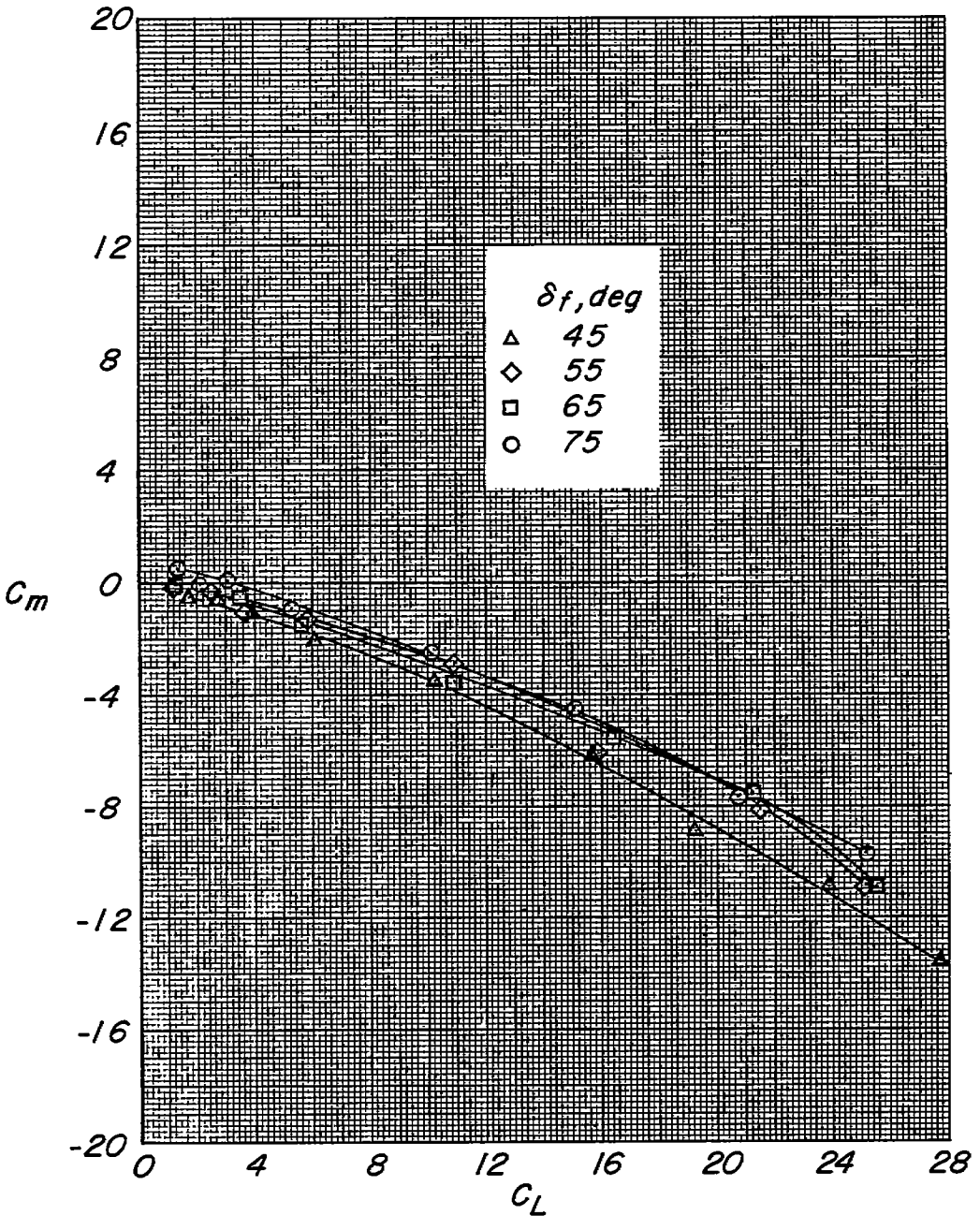

(c) Variation of C_m with C_L for various flap-deflection angles.

Figure 8.- Concluded.

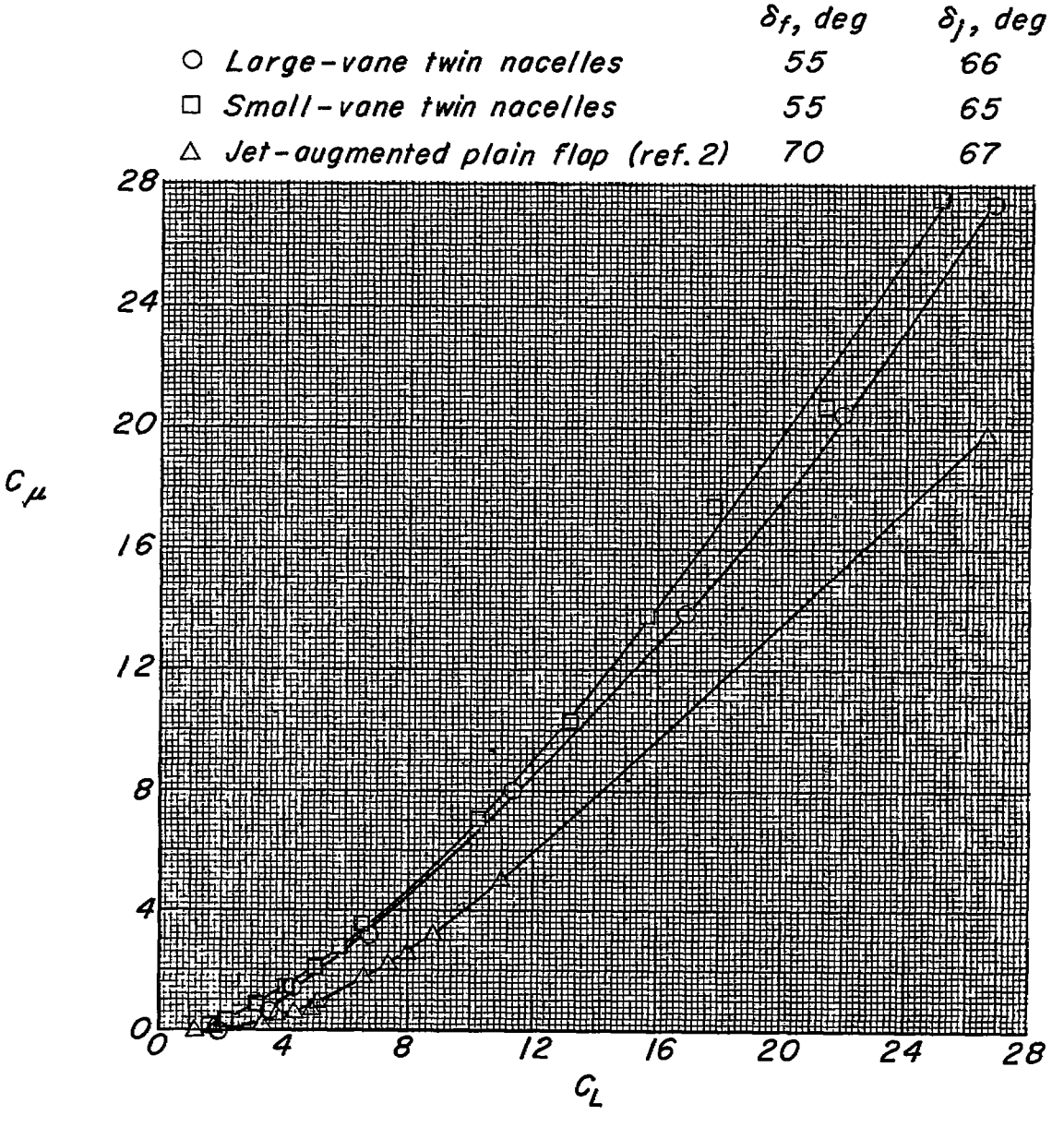

(a) Variation of C_μ with C_L.

Figure 9.- Comparison of aerodynamic characteristics of two external-flow jet-augmented double slotted flaps with a jet-augmented plain flap.

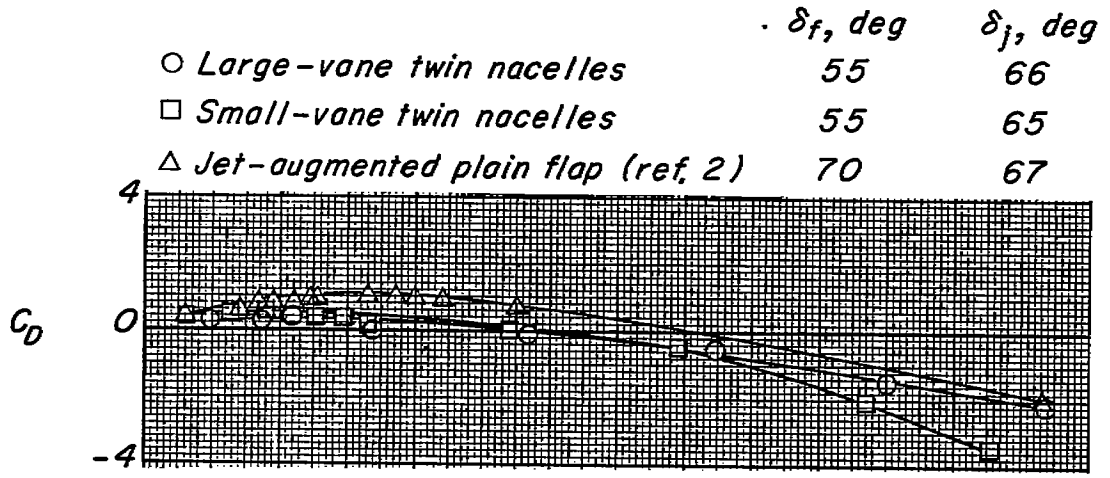

(b) Variation of C_D with C_L.

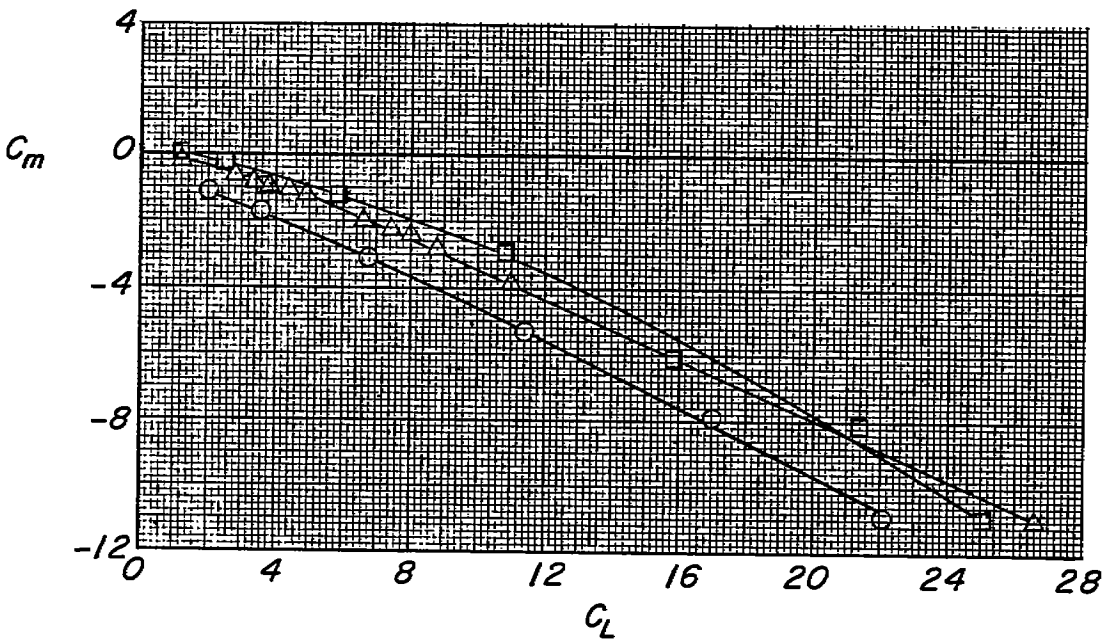

(c) Variation of C_m with C_L.

Figure 9.- Concluded.

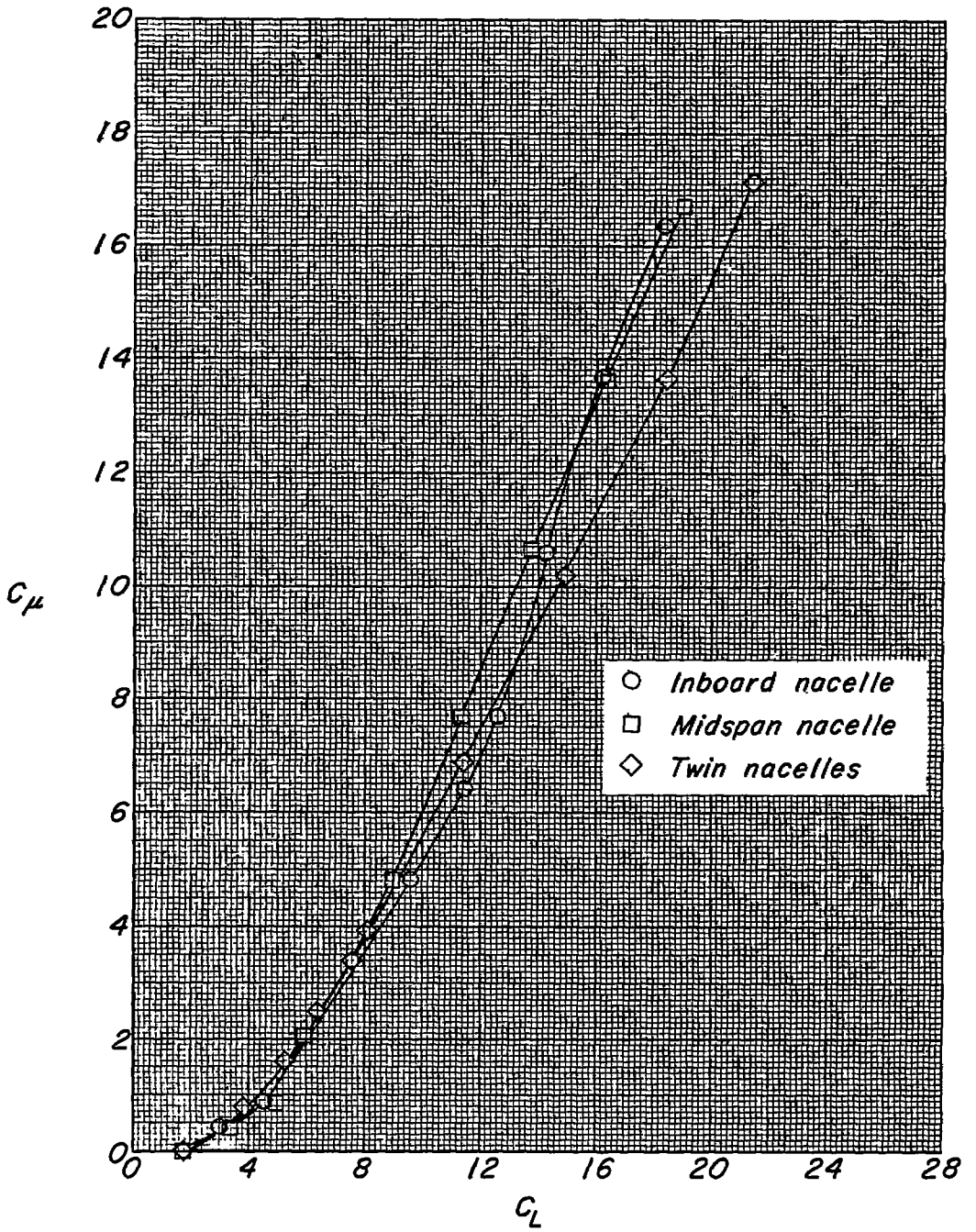

(a) Variation of C_μ with C_L.

Figure 10.- Aerodynamic effects of nacelle position and number on the large-vane configuration. $\alpha = 0°$; $\delta_f = 75°$.

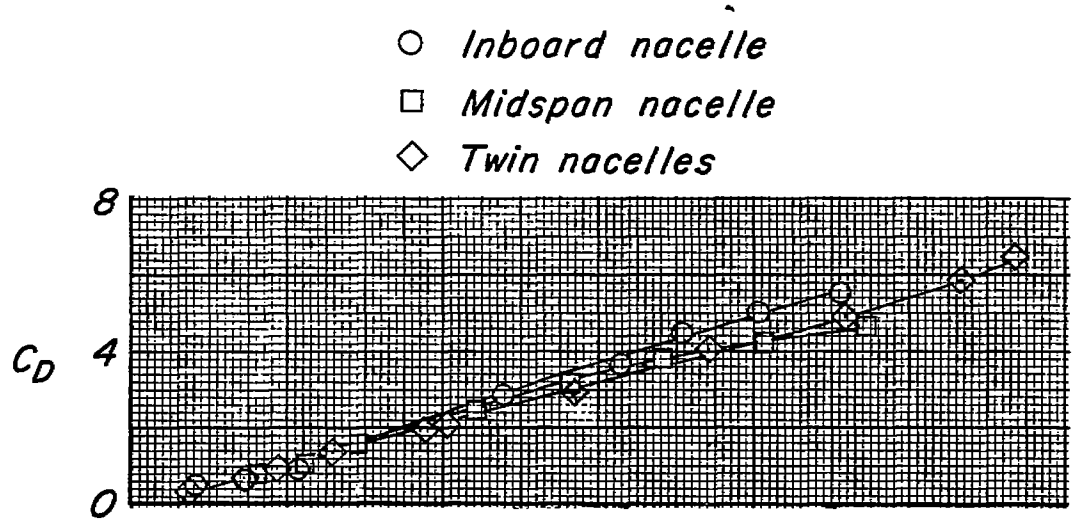

(b) Variation of C_D with C_L.

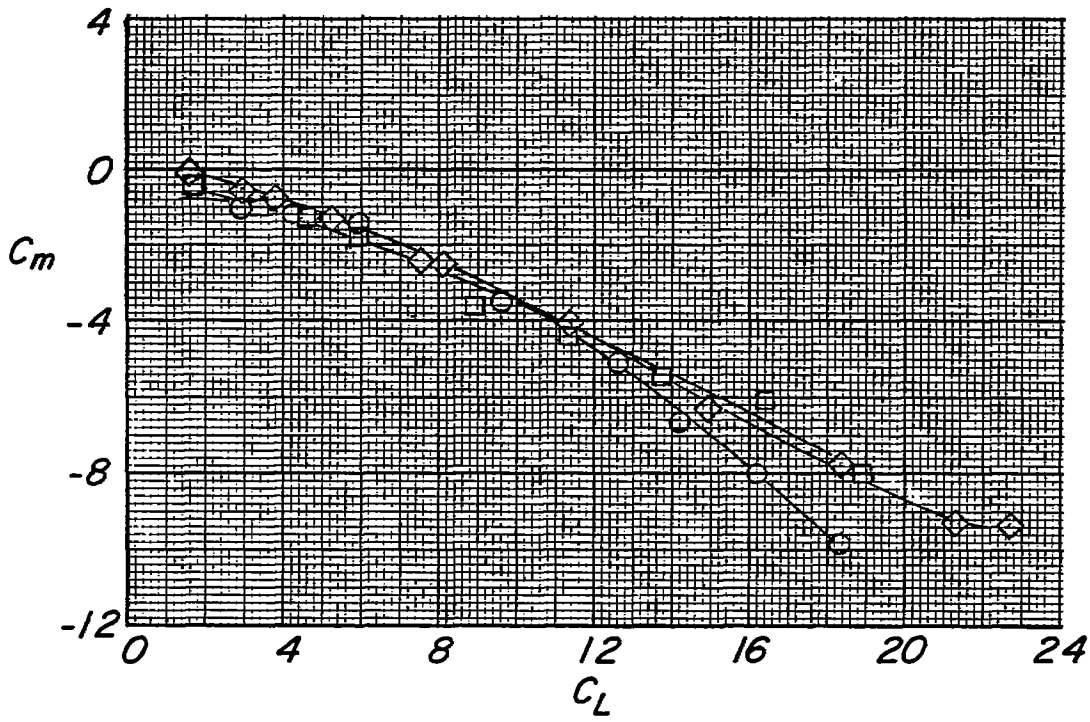

(c) Variation of C_m with C_L.

Figure 10.- Concluded.